Human Ecology
Online ISSN: 3041-9255
www.landscapeecologyjournals.ir

ORIGINAL ARTICLE
Vol. 5, Issue 14 (2026) | Article e244555
DOI: https://doi.org/10.22034/he.2026.583730.1217
Received: 29 Aug 2026 | Revised: 31 Oct 2026
Accepted: 25 Nov 2026 | Published: 28 Nov 2026

Article DOI

Assessment of the Effects of Social Vulnerability Indicators on Exposure and Physical Vulnerability

Mahnaz Keshavarz[1], Mohammad Mohammadi[2], Shayan Gadari[3], Abdolsalam Esmailzadeh[4,*]

[1] *Department of Geography, Faculty of Law and Social Sciences, Payame Noor University, Tehran, Iran.*

[2] *Department of Remote Sensing and GIS, Science and Research Branch, Islamic Azad University, Tehran, Iran.*

[3] *Department of Urban Planning, Islamic Azad University, Kerman, Iran.*

4 Department of Urban and Regional Planning, Allameh Tabataba'i University, Tehran, Iran.

*** Corresponding author:** Abdolsalam Esmailzadeh; a.esmailzadeh2000@gmail.com

ORCID: 0000-0002-4384-492X

Abstract

This research investigates the effects of social vulnerability indicators on exposure and physical vulnerability indicators in Masjed Soleyman, identified as a multi-hazard city. The study was carried out in three stages. In the first stage, the study identified and spatially analyzed natural and human-induced hazards, including floods, earthquakes, landslides, and oil pollution, and calculated a composite exposure indicator for the city's census tracts. In the second stage, we weighted and ranked social and physical vulnerabilities using multi-criteria decision-making techniques. In the third stage, the geographically weighted regression (GWR) model was used to examine the effects of social indicators, including household density, illiteracy rate, unemployment rate, and the proportion of rental housing units on exposure and physical vulnerability indicators across the study area's census tracts. The results indicate that the central and southern parts of the city have the highest exposure, while physical vulnerability is spatially dispersed across the city. In contrast, social vulnerability is most concentrated in the central and northern areas. The GWR results show that social indicators have a positive and significant effect on exposure and physical vulnerability. The findings can guide municipal and provincial authorities in designing targeted risk reduction strategies, optimizing resource allocation, and informing urban development decisions that consider social and physical vulnerabilities, while enhancing public awareness and fostering community engagement in hazard preparedness.

Keywords: Multi-Hazard Assessment; Social Vulnerability; Physical vulnerability; Risk Reduction; GIS

1. Introduction

Cities worldwide are growing rapidly, with populations increasing (Alam et al., 2018). Climate change (Bixler et al., 2021), hazards, and natural disasters are among the deadliest threats to people's lives and property in cities (Alam et al., 2018). The increase in the speed of disasters and hazards is such that documents and evidence show that cities have witnessed a significant increase in the occurrence of global disasters and their effects in the last two decades, and an increasing number of people have been affected by them, leading to substantial human and financial losses (Drakes & Tate, 2022a; Ebert et al., 2009). Some of the deadliest incidents include the 2010 Russian heat wave, Hurricane Katrina in 2005, the COVID-19 pandemic (Kalaycıoğlu et al., 2023), and Hurricane Maria in 2017 (Drakes & Tate, 2022a). Natural disasters in Asia, particularly earthquakes and floods in South Asia, are a serious problem (Khan et al., 2019), including Typhoon Nida in 2016 in China (Chen et al., 2023) and the 2011 earthquake and tsunami in Tohoku (Ba et al., 2021). Iran also has one of the highest rates of seismic activity in the world (Alizadeh, Alizadeh, Kotenaee, & Shahabi, 2018). Furthermore, earthquakes, floods, and fires occur in different cities across the country (Pourghasemi et al., 2020).

Accordingly, many urban areas are often affected by multi-hazard events. A multi-hazard incident refers to events that involve more than one natural disaster and are usually more devastating and impactful than a single-hazard event. This is because multi-hazard events can create overlapping effects and make it difficult for first responders to respond effectively (Xofi et al., 2022). Multi-hazard events describe the potential effects and outcomes of multiple hazards in a specific location. Landslides, floods, earthquakes, terrorism, industrial accidents, fires, financial crises, epidemics, and human-caused events like artificial explosions(Ghajari et al., 2017) or oil pollution(Bai et al., 2019; Fang et al., 2022) are a few examples of these hazards(Ferreira & Santos, 2023).

Moreover, hazards affect cities and regions differently. One hazard can trigger another through cascading effects. Two or more hazards can simultaneously hit a region or city (Depietri et al., 2018; Drakes & Tate, 2022a). In addition, hazards can affect a subject or object sequentially, leading to cumulative effects(Depietri et al., 2018). Meanwhile, the severity of hazards has a significant impact on life, livelihood, buildings, and infrastructure(Bixler et al., 2021)(Kappes et al., 2012). As such, urban areas worldwide suffer more casualties and economic losses because of population density, infrastructure, and assets, as well as inadequate management, making them more vulnerable (Depietri et al., 2018; Ferreira & Santos, 2023). Given this, multi-hazard risk assessment in urban areas can help reduce, manage, and mitigate the risks created by the combination of multiple natural disasters, as well as reduce the potential for loss of life and property damage (Mladineo et al., 2022). Natural hazards hitting a community with inadequate preparation can also cause significant damage to people and property and bring economic losses (Santos-Reyes, 2020). Thus, multi-hazard events have a more destructive impact in worn-out, historical contexts or in societies with spatial and social inequalities.

Accordingly, multi-hazard assessment is not only a frontier challenge for scientific studies but also has a major impact on the national economy, strategy, and people's lives (Ba et al., 2021). As such, hazard identification and understanding hazard types are critical for disaster risk reduction in areas with multiple simultaneous hazards and dynamic internal and external geographic processes (Aksha et al., 2020a; Ferreira & Santos, 2023; Sevieri et al., 2020; Zou et al., 2022). Moreover, vulnerability to multiple hazards differs across societies. Vulnerability involves different dimensions, including social vulnerability and physical/structural vulnerability. Social vulnerability refers to the increased likelihood that some populations will suffer negative hazard effects and reduced capacity to cope with them (Drakes & Tate, 2022b). Social vulnerability also describes the inherent characteristics of social systems that expose communities to more or less damage and shape their capacity to resist and recover from these effects (Guo et al., 2020). Physical vulnerability also involves housing and access characteristics. In other words, physical vulnerability (PV) refers to the characteristics of physical structures (e.g., materials and construction quality) that determine their potential damage in a disaster (Ebert et al., 2009). Given the importance of multi-hazard assessment, several studies have examined multiple hazards in cities and assessed community vulnerability across different dimensions (Amini et

al., 2023; Chen et al., 2023; Gentile et al., 2022; Pourghasemi et al., 2020; Rusk et al., 2022). For example, some studies have focused on social vulnerability to earthquakes (Alam et al., 2018; Alizadeh, Alizadeh, Kotenaee, Shahabi, et al., 2018; Guo et al., 2020). Hadipour et al. investigated social indicators related to sea-level rise and flooding (Hadipour et al., 2020). Mengal et al. 2021) examined social vulnerability assessment against earthquakes and tsunamis. Some have also investigated the physical vulnerability to tremors in residential areas (Alam et al., 2018; Khan et al., 2019). Moreover, several studies have addressed physical or social vulnerability in multi-hazard cities. For example, Gentile et al. (2022) and Kappes et al. (2012) evaluated physical vulnerability across multiple hazards. Other studies (Drakes & Tate, 2022b; Kalaycıoğlu et al., 2023; Zhang et al., 2023) have also investigated social vulnerability to multi-hazard events. Although many studies have addressed physical and social aspects of vulnerability, little effort has been made to measure Physical and social vulnerability in a multi-hazard city. Furthermore, one innovation of the present research compared with previous studies is the analysis of man-made hazards such as oil pollution.

Masjed Soleyman, a city in southwest Iran near the Persian Gulf, faces a wide variety of natural and human hazards. This region faces risks such as floods from overflowing rivers and landslides (Mousavi et al., 2020) and, as one of Iran's active seismic regions, strong earthquakes (Safari et al., 2010). In addition, Khuzestan Province experiences extensive drought periods and water shortages, along with flood potential (Ahmadi et al., 2022; Khavarian-Garmsir et al., 2019). Furthermore, the presence of oil and gas industries in this area increases the risk of industrial accidents and chemical pollutants. As the population grows and villagers migrate to Masjed Soleyman, more people are living in high-risk areas (Sani et al., 2015), increasing hazards across the city. In other words, changes in demographic patterns and migration to high-risk areas have increased the need for special attention to managing and reducing these risks.

Using spatial, physical, and social data, the present research aimed to help local decision-makers and policymakers develop effective risk mitigation plans. This research introduces an integrated approach to multi-hazard risk assessment in Masjed Soleyman. First, it provides single-hazard assessments of earthquakes, floods, landslides, and oil pollution. Then, it calculates social and Physical vulnerability indices for Masjed Soleyman. Finally, it integrates the findings to present a multi-hazard assessment of Masjed Soleyman. In addition, this research adopts a spatial approach and multi-criteria decision-making methods to analyze and evaluate different hazards in the city. The insights from this research may inform local decision-making and policy on risk reduction and management in Masjed Soleyman.

2. Materials and methods

2.1. Study area

Masjed Soleyman, with an area of 1922 hectares, is the capital of Masjed Soleyman County and is located at 31.5230°-32.0145° N and 49.1135°-49.1420° E in northeast Khuzestan Province, Iran. The city's average elevation is 376 meters above sea level. The city has a hot, dry climate, and average air temperatures exceed 42°C for seven months of the year (Kassiri et al., 2014). Because of its geographical features, Masjed Soleyman faces many problems. Given the location of the oil field and also the presence of many abandoned wells in some areas of the city, gas emissions from the land surface have endangered the lives of citizens and even led to the death of some of the city's residents. Parts of the city are contaminated by subsurface natural gas leaks containing high concentrations of H2S and other sulfur compounds. Thus, this pollution has affected the sex ratio of children in families, blood changes and blood pressure changes, and suicide among people living in the polluted area (Saadat et al., 2004, 2006). Constructions have been erected on steep slopes (up to 30%) in some areas of the city, and these slopes have loose soil, leading to human and financial losses due to slope movements and landslides. Furthermore, the southern parts of the city are in a very high-vulnerability zone due to the fault's passage, and the central parts of the city are also in a high-risk zone. Figure 1 shows an integrated map of the hazards in Masjed Soleyman:

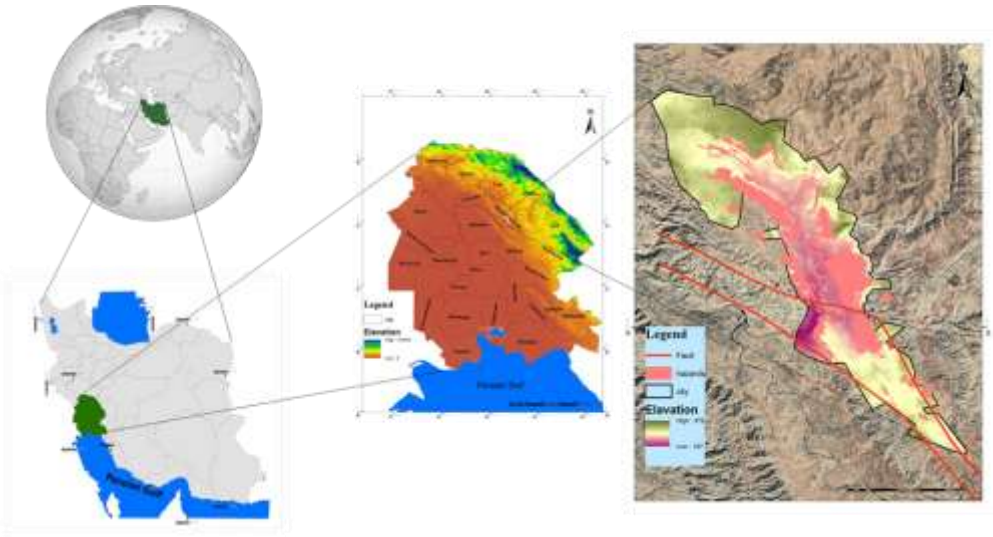

Fig. 1. Location of Masjed Soleyman

2.2. Data and analysis methods

To meet the research objectives, this study used multi-criteria decision-making methods and GIS to display and describe hazards and physical and social variables in Masjed Soleyman. The unit of analysis was Census Tracts in Masjed Soleyman. This research was conducted in two phases. In the first phase, the study analyzed the most frequent hazards affecting the city, such as floods, earthquakes, and landslides. The second phase of the research analyzed the Physical and social vulnerability of the city. This research adopted a spatial approach to multi-hazard assessment. Advantages of this approach include spatial accuracy, result sharing, computing capacity, and increased inputs (Aksha et al., 2020b).

2.2.1. Data collection

The data in this research were collected in two stages. In the first stage, the data related to hazards in Masjed Soleyman were collected. These data focused on landslide areas, oil-polluted areas, and flood areas, and seismicity rates prepared by the Geological Survey and Mineral Exploration of Iran, the Housing and Urban Development Organization, and Khuzestan Governorate. We extracted physical and social vulnerability data for census tracts in Masjed Soleyman from the Statistical Center of Iran. We prepared the hazard data as GIS layers and, after editing, estimated the ratio of each hazard in the statistical areas. We also calculated the ratio of placement in the seismic zones. We measured seismicity zoning as a three-part spectrum in the city. Each spectrum was given a code. Then, we multiplied each zone's ratio by its code and calculated the seismicity percentage. The statistical areas were raw data and were converted into indices and ratios in ArcGIS software.

2.2.2. Indicators

The intended indicators were extracted after reviewing the social vulnerability literature. The indicators were screened according to data availability. Finally, 4 indicators were selected to investigate Physical vulnerability, and 9 indicators were specified to investigate social vulnerability, as detailed in Table 1

Table 1. Physical and social vulnerability and exposure indicators

Dimension	Indicator	Description	References
Physical vulnerability	Building type	Increasing	(Alizadeh, Alizadeh, Kotenaee, & Shahabi, 2018; Shadmaan & Popy, 2023; P. K. Thakur et al., 2012)
	Construction materials	Increasing	(Alizadeh, Alizadeh, Kotenaee, & Shahabi, 2018; Shadmaan & Popy, 2023)
	Building area	Increasing	(Alizadeh, Alizadeh, Kotenaee, & Shahabi, 2018; Chakraborty et al., 2020)
	Building frame	Increasing	(Alizadeh, Alizadeh, Kotenaee, & Shahabi, 2018)
Social vulnerability	Literacy	Decreasing	(Dintwa et al., 2019; Ikram et al., 2023; Waly et al., 2021)
	Population density	Increasing	(Aksha et al., 2020b; de Loyola Hummell et al., 2016; Lee, 2014; Morales & Vries, 2021)
	Household density	Increasing	(Fatemi et al., 2017)(Alizadeh, Alizadeh, Kotenaee, & Shahabi, 2018)(Tasnuva et al., 2021)(Dintwa et al., 2019)
	Female population	Increasing	Fatemi et al.,2017; Aksha et al.,2019; Dwyer et al.,2004; Yoon,2012
	Children's population	Increasing	Waly et al.,2021; Fatemi et al.,2017; Cutter et al.,2012; Flanagan et al.,2011
	Unemployment rate	Increasing	Waly et al.,2021; Aksha et al.,2019; Bergstrand et al.,2015; Rufat et al.,2015
	Rental rate	Increasing	Maso et al.,20121; Van Zandt et al., 2012
	Population over 65 years old	Increasing	Waly et al., 2021; Fatemi et al.,2017; de Loyola Hummell,2016; Flanagan et al.,2011
	Female-headed households	Increasing	Aksha et al.,2019; de Loyola Hummell,2016
Exposure	Earthquake	Seismicity ratio	
	Flood	Flooding zones	
	Landslide	Landslide areas	
	Oil pollution	Oil-polluted areas	

2.2.3. Analysis procedures

This study was conducted in three stages. In the first stage, we identified and spatially analyzed natural and human-induced hazards in Masjed Soleyman. We used ArcGIS software to derive a composite exposure indicator. In this stage, we calculated each hazard's proportion relative to the total area of the census tracts and standardized the data to a range of zero to one for comparability. Next, we spatially overlaid the hazard layers to derive the final exposure indicator.

In the second stage, we assessed and ranked social and physical vulnerability indicators across the census tracts. This stage employed a multi-criteria decision-making (MCDM) approach. The Best–Worst Method (BWM) weighted the indicators, and the Compromise Ranking of Order of Preference by Similarity to Ideal Solution (COCOSO) method produced the final ranking. We extracted the required data from the national census results and entered them into the model as the initial matrix. In the COCOSO model, we considered 69 census tracts as alternatives and used 4 physical and 9 social indicators as criteria.

Because each indicator's importance and impact vary, the BWM method first determined indicator weights based on the opinions of six local experts and managers. These weights were then applied in the COCOSO model to derive the final ranking of each block by social and physical vulnerability. This stage produced final maps and tables showing vulnerability levels across different areas of the city.

In the third stage, the geographically weighted regression (GWR) model was used to analyze the relationship between social vulnerability indicators and physical vulnerability and exposure indicators. This model is preferred over the classical linear regression model because it captures spatial heterogeneity in local relationships. In this analysis, the physical vulnerability and exposure indicators were considered as dependent variables. In contrast, social indicators including household density, unemployment rate, illiteracy rate, and the proportion of rental housing units were treated as independent variables.

The GWR model examined spatial variation in how social indicators affected physical vulnerability and exposure across urban areas. To evaluate the model's performance, we calculated metrics such as bandwidth, residual sum of squares (RSS), coefficient of determination (R^2), and corrected Akaike Information Criterion (AICc). Ultimately, the model's local coefficients indicated the magnitude and direction of each social indicator's effect on physical vulnerability across different parts of the city.

3. Results

3.1. Hazard exposure assessment

3.1.1. Earthquake

Masjed Soleyman was divided into three zones of very high, high, and relatively high seismic risk, coded accordingly, and the final seismicity ratio was calculated. In a very high-risk area, 100% of the city is earthquake-prone. However, the seismic risk is lower in other areas.

3.1.2. Landslide

We calculated the proportion of landslide zones in each statistical area. Area No. 56 has the highest ratio, and the northern areas have no landslides because of the lower slope, so the landslide ratio is zero. The central and western areas of the city have the most frequent landslide zones, while the northern and southern areas have the lowest landslide risk.

3.1.3. Flooding

Currently, 10 valleys (flood channels) totaling 33 km run across the city and carry floods, surface water, and domestic and industrial sewage. The ratio of these channels varies across different areas. Area No. 39 has the highest ratio, while the southern parts of the city have the lowest.

3.1.4. Oil pollution

Another problem in Masjed Soleyman is the presence of oil and gas resources, which has caused many accidents in the city. Many residential units have been built in the vicinity of oil and gas wells, creating many environmental problems in the city and causing poisoning and blood pressure disorders for the residents. Pollution from oil and gas wells affects parts of the southeast and the city center. Two oil and gas spill-contaminated regions cover an area of about 356.6 hectares in the southeast of the city and 6.6 hectares in the central part of the city (363.2 hectares in total), of which about 1,287 hectares are located within the city boundaries, as shown in Figure 2:

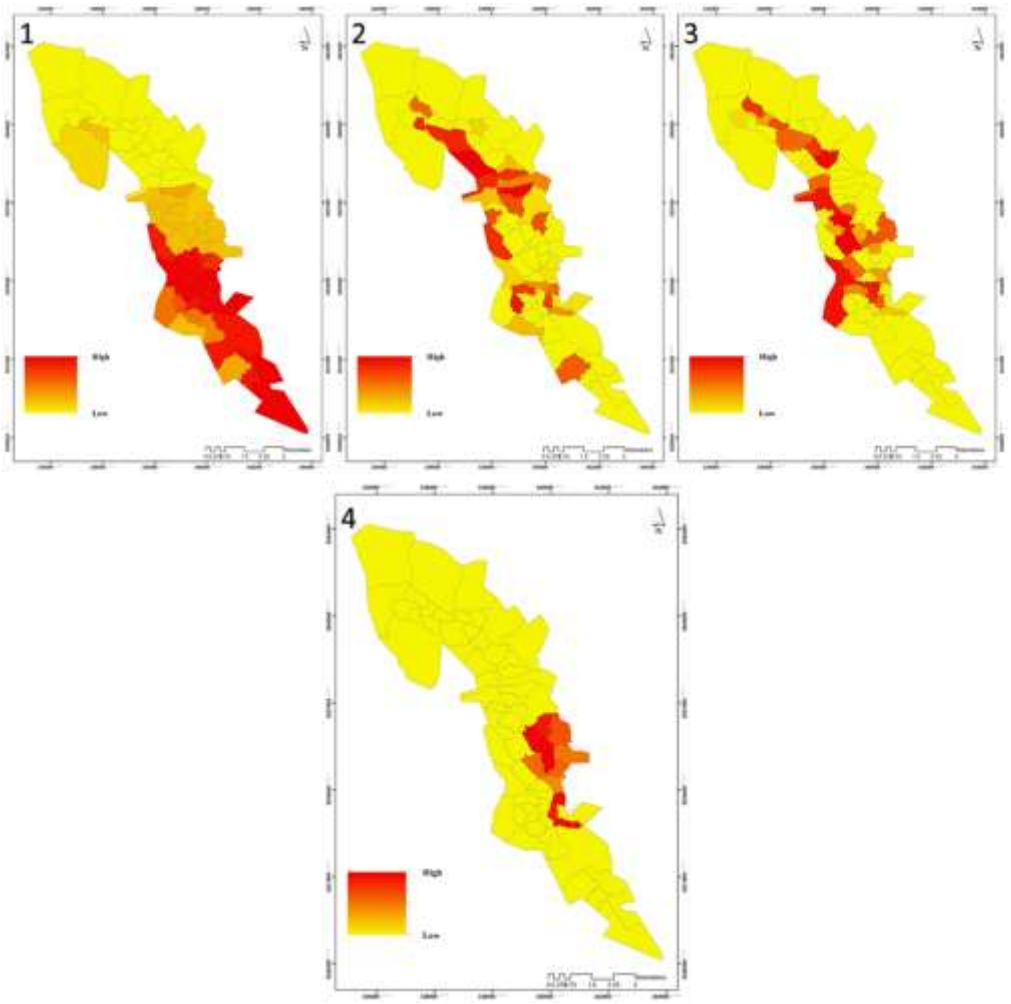

Fig. 2. Spatial representation of hazards in different areas of Masjed Soleyman: (1) Earthquake, (2) landslide, (3) flood, and (4) oil pollution

We plotted the exposure map by superimposing the standardized hazard maps for earthquake, landslide, flood, and oil pollution (Figure 3). Census Tract No. 10 has the highest exposure, and Census Tract No. 59 has the lowest. As shown in Figure 4, the central parts of the city have the highest exposure to hazards. These areas are most affected by earthquakes, oil pollution, and floods, while the northern parts (blue areas) are less frequently exposed to hazards.

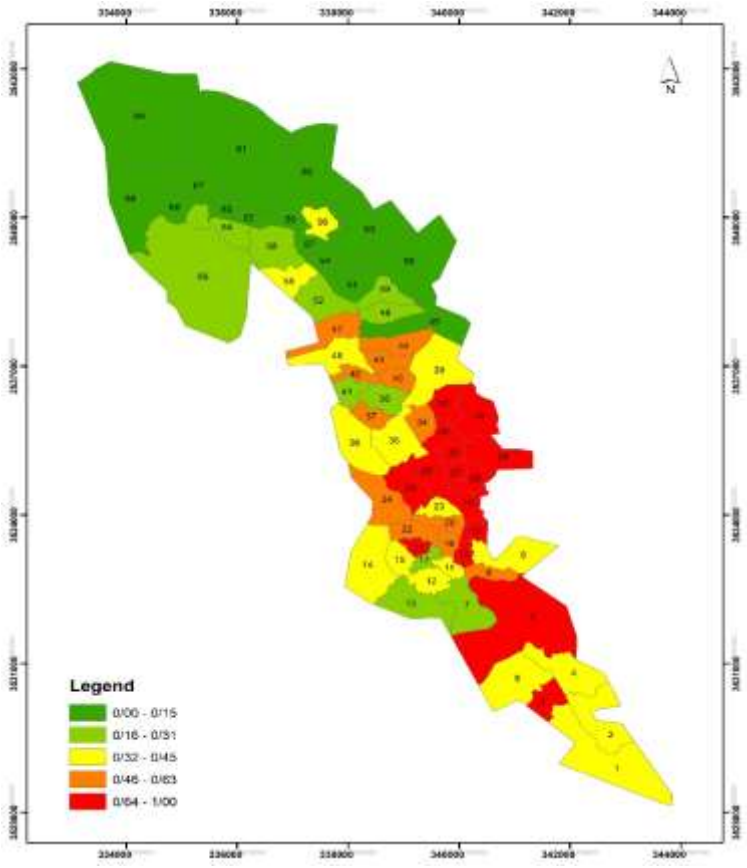

Fig. 3. Hazard zoning of different Census Tracts of Masjed Soleyman

3.2. Physical vulnerability assessment

To zone and rank the city's Census Tracts based on four indicators, we used the multi-criteria decision-making (MCDM) technique. Because indicators differ in importance, we applied the BWM weighting model. The building frame had the highest weight, while the building type had the lowest.

Next, we ranked the city's statistical areas using the COCOSO model, as detailed in Table 2. We multiplied the weights from this model by the indicators. The model included 69 Census Tracts as alternatives and used social vulnerability indicators as criteria. We ranked the areas from highest to lowest physical vulnerability. The highest score indicates the greatest physical vulnerability, with Census Tract No. 19 having the highest and Census Tract No. 37 having the

Table 2. The ranks of the Census Tracts in terms of Physical vulnerability indicators

Area code	Ka	Kb	Kc	k	Area code	Ka	Kb	Kc	k
1	0.0165	6.5514	0.9256	2.9620	37	0.0113	2.0000	0.6330	1.1240
2	0.0142	4.4717	0.7983	2.1318	38	0.0131	3.8002	0.7351	1.8482
3	0.0152	5.0753	0.8515	2.3839	39	0.0131	3.3082	0.7337	1.6683
4	0.0143	4.1542	0.8022	2.0194	40	0.0122	2.5414	0.6830	1.3553
5	0.0149	4.6363	0.8339	2.2142	41	0.0131	3.7895	0.7362	1.8450
6	0.0155	5.0337	0.8711	2.3818	42	0.0120	2.3621	0.6759	1.2846
7	0.0130	3.0810	0.7295	1.5825	43	0.0135	3.3252	0.7555	1.6881
8	0.0176	8.9451	0.9869	3.8540	44	0.0138	3.5664	0.7717	1.7864
9	0.0137	3.9993	0.7711	1.9434	45	0.0157	5.5385	0.8834	2.5714
10	0.0151	4.8502	0.8451	2.2987	46	0.0158	6.0381	0.8862	2.7522
11	0.0144	4.2853	0.8073	2.0702	47	0.0128	2.8179	0.7165	1.4779
12	0.0147	4.3045	0.8237	2.0877	48	0.0142	4.2938	0.7977	2.0671
13	0.0169	6.5428	0.9471	2.9734	49	0.0160	6.5241	0.9004	2.9353

Area code	Ka	Kb	Kc	k	Area code	Ka	Kb	Kc	k
14	0.0150	4.4440	0.8401	2.1487	50	0.0135	3.5336	0.7593	1.7666
15	0.0131	2.7829	0.7370	1.4774	51	0.0119	2.2305	0.6670	1.2303
16	0.0140	4.1948	0.7869	2.0243	52	0.0139	3.9167	0.7810	1.9197
17	0.0155	5.1178	0.8712	2.4121	53	0.0141	4.2575	0.7925	2.0506
18	0.0139	3.8491	0.7795	1.8942	54	0.0126	2.8259	0.7096	1.4765
19	0.0229	16.4223	1.2837	6.6939	55	0.0143	4.2264	0.8012	2.0450
20	0.0126	2.8043	0.7087	1.4680	56	0.0167	6.9160	0.9370	3.0998
21	0.0132	3.0417	0.7432	1.5766	57	0.0150	4.8744	0.8388	2.3033
22	0.0136	3.6934	0.7631	1.8272	58	0.0130	3.0418	0.7304	1.5687
23	0.0175	8.2359	0.9807	3.5987	59	0.0156	5.5373	0.8771	2.5668
24	0.0150	4.5775	0.8431	2.1989	60	0.0157	5.5441	0.8804	2.5714
25	0.0142	3.9665	0.7942	1.9462	61	0.0132	3.1654	0.7424	1.6215
26	0.0150	4.6905	0.8398	2.2376	62	0.0157	5.8581	0.8808	2.6842
27	0.0158	4.8175	0.8861	2.3135	63	0.0160	6.7609	0.8953	3.0162
28	0.0160	5.9094	0.8979	2.7140	64	0.0133	3.3881	0.7488	1.7069
29	0.0153	4.3333	0.8559	2.1187	65	0.0127	3.6558	0.7145	1.7827
30	0.0150	4.1329	0.8392	2.0353	66	0.0119	2.4131	0.6694	1.2996
31	0.0161	6.4149	0.9054	2.8997	67	0.0134	3.7821	0.7520	1.8524
32	0.0159	5.9310	0.8934	2.7187	68	0.0143	5.0215	0.8030	2.3327
33	0.0157	6.2063	0.8825	2.8099	69	0.0141	4.9777	0.7928	2.3102
34	0.0126	2.9335	0.7091	1.5158	37	0.0113	2.0000	0.6330	1.1240
35	0.0131	3.4563	0.7357	1.7236					
36	0.0152	4.6949	0.8529	2.2477					

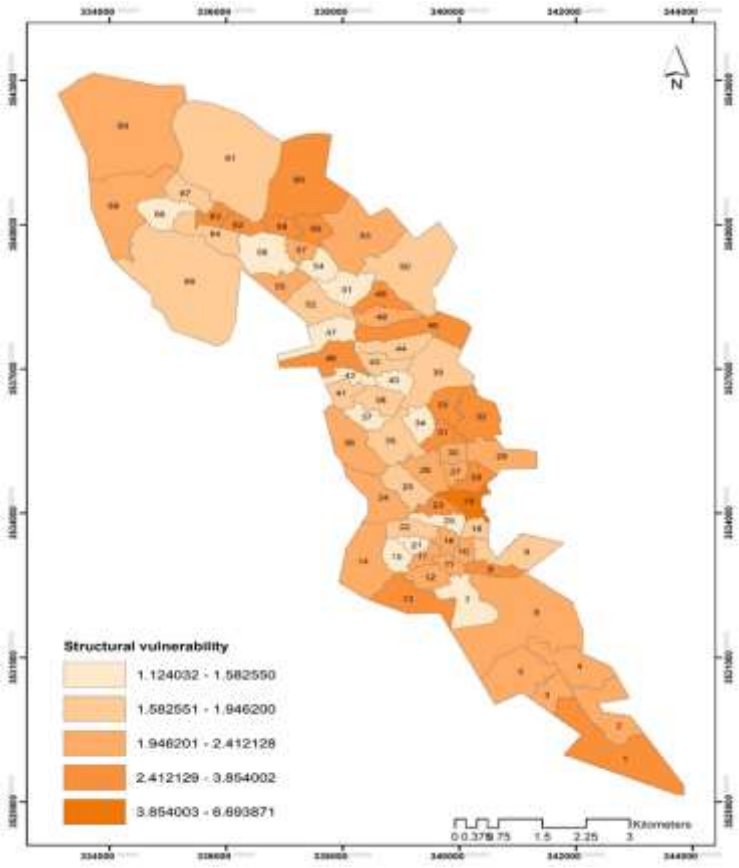

Fig. 4. The spatial representation of Physical vulnerability in different Census Tracts

3.3. Social vulnerability assessment

As with physical vulnerability, we evaluated social vulnerability in Masjed Soleyman using the COCOSO technique and the BWM weighting model. Nine indicators measured social vulnerability, and we assessed their relative importance. The results showed that population density had the highest weight, confirming its significant role in the city's social vulnerability, while the rental rate had the lowest weight, indicating minimal impact.

The model used 69 Census Tracts as alternatives, and the indicators served as criteria. The outputs ranked the areas from the highest to the lowest social vulnerability. Census Tract No. 17 showed the highest social vulnerability, whereas Census Tract No. 65 exhibited the lowest(Table 3). Figure 5 illustrates the spatial distribution of social vulnerability across the Census Tracts.

Table 3. The ranks of the Census Tracts in terms of social vulnerability indicators

Area code	Ka	Kb	Kc	k	Area code	Ka	Kb	Kc	k
1	0.01378	1.48166	0.86464	1.04707	36	0.01422	1.46769	0.89199	1.05630
2	0.01403	1.50792	0.88016	1.06574	37	0.01555	2.42390	0.97592	1.47105
3	0.01477	1.71054	0.92654	1.16999	38	0.01462	1.61548	0.91745	1.12798
4	0.01433	1.46187	0.89902	1.05778	39	0.01391	1.24401	0.87305	0.95755
5	0.01404	1.33747	0.88100	0.99898	40	0.01525	2.14771	0.95677	1.35517
6	0.01339	1.25648	0.84013	0.94511	41	0.01489	1.81056	0.93416	1.21297
7	0.01420	1.39463	0.89118	1.02704	42	0.01540	2.26307	0.96603	1.40437
8	0.01521	2.05696	0.95453	1.31917	43	0.01526	2.11006	0.95770	1.34128
9	0.01416	1.41601	0.88828	1.03394	44	0.01476	1.71935	0.92628	1.17327
10	0.01565	2.36359	0.98202	1.45160	45	0.01445	1.60977	0.90686	1.12001
11	0.01568	2.40758	0.98416	1.46952	46	0.01421	1.41730	0.89193	1.03640
12	0.01491	1.83206	0.93551	1.22203	47	0.01460	1.66455	0.91637	1.14654
13	0.01277	1.53198	0.80149	1.03239	48	0.01520	1.98694	0.95388	1.29190
14	0.01377	1.39374	0.86387	1.01210	49	0.01488	1.76285	0.93351	1.19412
15	0.01509	1.92841	0.94701	1.26557	50	0.01400	1.51320	0.87836	1.06683
16	0.01577	2.43339	0.98974	1.48247	51	0.01460	1.61908	0.91628	1.12875
17	0.01594	2.56299	1.00000	1.53736	52	0.01461	1.62578	0.91669	1.13159
18	0.01535	2.14207	0.96304	1.35651	53	0.01370	1.27107	0.85956	0.96122
19	0.01468	1.68328	0.92099	1.15636	54	0.01478	1.78952	0.92750	1.20117
20	0.01512	1.93213	0.94892	1.26806	55	0.01481	1.75692	0.92957	1.18966
21	0.01567	2.40751	0.98336	1.46904	56	0.01514	1.94841	0.95029	1.27509
22	0.01492	1.84521	0.93612	1.22745	57	0.01532	2.09736	0.96104	1.33827
23	0.01535	2.13836	0.96319	1.35517	58	0.01422	1.42195	0.89200	1.03827
24	0.01400	1.28390	0.87840	0.97630	59	0.01514	1.96006	0.95001	1.27943
25	0.01463	1.60174	0.91770	1.12275	60	0.01344	1.15310	0.84344	0.90556
26	0.01238	1.32967	0.77678	0.94011	61	0.01508	1.99593	0.94647	1.29126
27	0.01579	2.44315	0.99108	1.48693	62	0.01349	1.42138	0.84650	1.01365
28	0.01530	2.06224	0.95990	1.32418	63	0.01576	2.52436	0.98890	1.51645
29	0.01445	1.67132	0.90689	1.14403	64	0.01512	1.94245	0.94852	1.27182
30	0.01571	2.36962	0.98572	1.45598	65	0.00932	1.00000	0.58465	0.70727
31	0.01520	2.02878	0.95403	1.30807	66	0.01464	1.74069	0.91835	1.17724
32	0.01429	1.50296	0.89679	1.07275	67	0.01480	1.83848	0.92876	1.22081
33	0.01492	1.83704	0.93613	1.22430	68	0.00990	1.20903	0.62126	0.80859
34	0.01524	2.03427	0.95611	1.31133	69	0.01008	1.46910	0.63276	0.91483
35	0.01436	1.44469	0.90095	1.05204					
36	0.01422	1.46769	0.89199	1.05630					

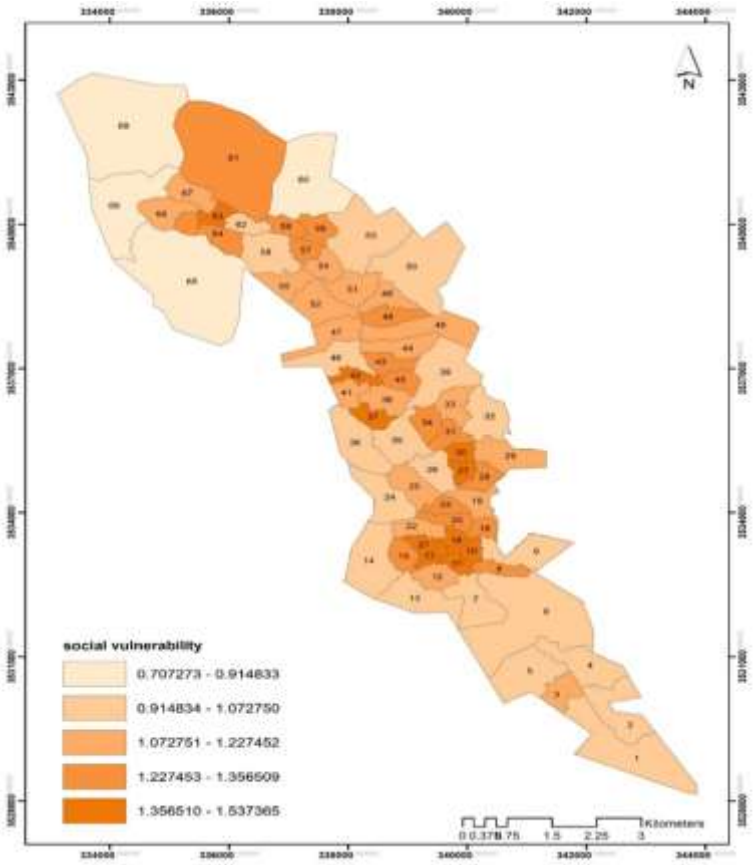

Fig. 5. The spatial representation of social vulnerability in different Census Tracts

Table 4 shows the overall assessment of exposure and Physical and social vulnerability in Masjed Soleyman. The rank of each area was calculated based on the final COCOSO indicators for Physical and social vulnerability and by superimposing flood, landslide, earthquake, and oil pollution maps. These indicators were then merged into the composite hazard map, and the final rank for each area was estimated.

Table 4. The exposure, Physical vulnerability, and social vulnerability rank for each Census Tract

Exposure				Physical vulnerability				Social vulnerability				Composite risk index			
Tract	Rank	Tract	Rank	Tract	Rank	Tract	Rank	Tract	Rank	Tract	Rank	Tract	Rank	Tract	Rank
1	29	37	46	1	7	37	69	1	52	37	5	1	34	37	27
2	23	38	24	2	31	38	46	2	48	38	43	2	63	38	47
3	37	39	45	3	19	39	55	3	37	39	63	3	28	39	66
4	27	40	22	4	40	40	65	4	49	40	13	4	64	40	20
5	36	41	35	5	28	41	47	5	60	41	31	5	57	41	37
6	32	42	26	6	20	42	67	6	64	42	10	6	53	42	19
7	47	43	33	7	57	43	54	7	57	43	14	7	65	43	29
8	8	44	9	8	2	44	49	8	17	44	36	8	1	44	38
9	15	45	55	9	42	45	16	9	55	45	45	9	56	45	31
10	1	46	25	10	25	46	11	10	9	46	54	10	4	46	30
11	18	47	13	11	34	47	61	11	6	47	39	11	24	47	40
12	51	48	53	12	33	48	35	12	29	48	20	12	44	48	35
13	41	49	58	13	6	49	8	13	56	49	33	13	36	49	13
14	21	50	66	14	30	50	51	14	59	50	47	14	59	50	68
15	7	51	54	15	62	51	68	15	26	51	42	15	26	51	49
16	6	52	16	16	39	52	43	16	4	52	41	16	14	52	48
17	38	53	67	17	18	53	36	17	1	53	62	17	11	53	69
18	10	54	57	18	44	54	63	18	11	54	32	18	12	54	42
19	11	55	17	19	1	55	37	19	38	55	34	19	2	55	39

Exposure				Physical vulnerability				Social vulnerability				Composite risk index			
Tract	Rank	Tract	Rank	Tract	Rank	Tract	Rank	Tract	Rank	Tract	Rank	Tract	Rank	Tract	Rank
20	2	56	59	20	64	56	4	20	25	56	23	20	17	56	10
21	19	57	62	21	58	57	24	21	7	57	15	21	25	57	18
22	3	58	43	22	48	58	59	22	27	58	53	22	23	58	58
23	14	59	69	23	3	59	17	23	12	59	22	23	5	59	16
24	4	60	63	24	29	60	15	24	61	60	67	24	50	60	54
25	12	61	64	25	41	61	56	25	44	61	21	25	45	61	43
26	31	62	60	26	27	62	14	26	65	62	58	26	52	62	41
27	39	63	65	27	22	63	5	27	3	63	2	27	9	63	7
28	34	64	20	28	13	64	53	28	16	64	24	28	6	64	33
29	48	65	52	29	32	65	50	29	40	65	69	29	46	65	67
30	50	66	61	30	38	66	66	30	8	66	35	30	15	66	55
31	42	67	49	31	9	67	45	31	19	67	30	31	3	67	32
32	40	68	56	32	12	68	21	32	46	68	68	32	22	68	60
33	28	69	68	33	10	69	23	33	28	69	66	33	8	69	62
34	44			34	60			34	18			34	21		
35	30			35	52			35	51			35	61		
36	5			36	26			36	50			36	51		

As shown in Table 4 and Figure 6, Census tract No. 8 has the highest level of risk, and Census tract No. 53 has the lowest level of risk (last rank). The central census tracts in the city have the highest exposure to hazards, while the northeastern and northwestern census tracts have the lowest.

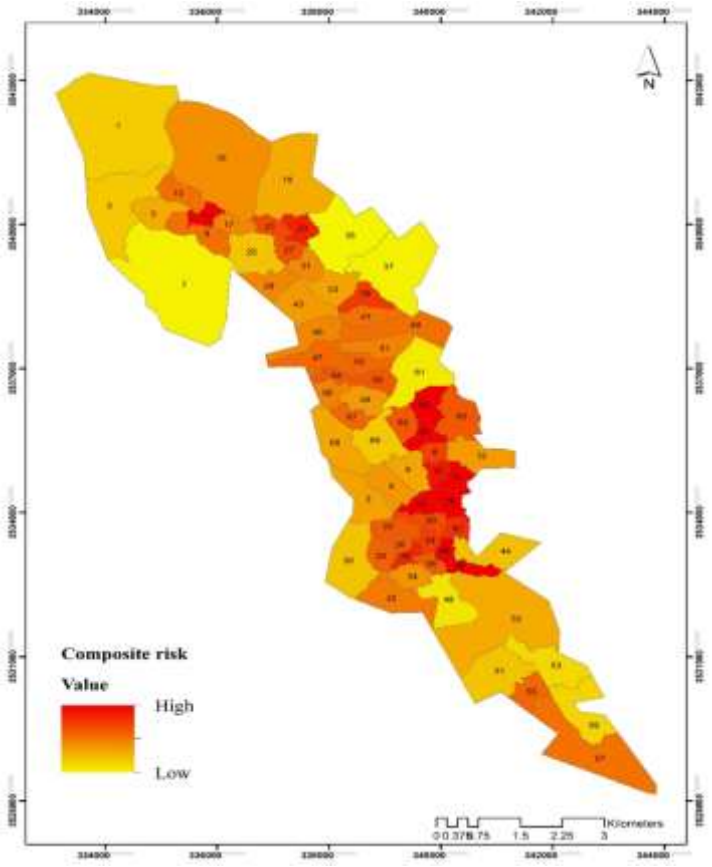

Fig. 6. The composite risk map

3.4. Assessment of the effects of social vulnerability indicators on physical vulnerability using the GWR model

To assess the impact of social vulnerability indicators on physical vulnerability in Masjed Soleyman, the geographically weighted regression (GWR) model was employed. Table 5 presents the model's statistical indicators, while Table 6 shows the local coefficients of the explanatory variables.

Table 5. Statistical Indicators of the GWR Model

Model Indicator	Value
Bandwidth	4957.22
Residual Sum of Squares (RSS)	0.0662
Effective Number of Parameters	11.58
Residual Standard Deviation (Sigma)	0.0339
Corrected Akaike Information Criterion (AICc)	-258.88
Coefficient of Determination (R^2)	0.536
Adjusted R^2	0.450

Table 6. Local Coefficients of the GWR Model Examining the Effects of Social Vulnerability Indicators on Physical Vulnerability

Variable	Coefficient Direction	Coefficient Range	Notes
Household Density	Positive / Negative	-0.0072 – 0.4156	The effect of household density varies across census tracts; in some areas, higher density increases the indicator, while in others it decreases it.
Illiteracy Rate	Negative	-0.0055 – -0.0018	Higher illiteracy generally decreases physical vulnerability across most tracts.
Unemployment Rate	Positive	0.00003 – 0.482	Higher unemployment increases the physical vulnerability indicator.
Proportion of Rental Units	Positive / Negative	-0.342 – 0.298	Mixed effect; in some tracts, an increase in rental units decreases the indicator, while in others it increases it.

The GWR results indicate that in areas with higher social vulnerability, the physical vulnerability indicator also shows significant increases or decreases; in other words, social conditions and urban physical fragility are significantly spatially related. In this model, the dependent variable is the census-tract-level physical vulnerability indicator. In contrast, the independent variables include household density, illiteracy rate, unemployment rate, and the proportion of rental housing units.

The model explained about 53% of the spatial variation in the physical vulnerability indicator (R^2 = 0.536), and the adjusted R^2 (0.450) indicates a good fit after accounting for the number of variables.

The indicator coefficients reflect the varying effects of social indicators. Household density exhibits both positive and negative effects across different census tracts, highlighting local differences in its impact on the physical vulnerability indicator. Illiteracy generally has a negative effect in most tracts, with higher illiteracy leading to a decrease in physical vulnerability. Unemployment shows a positive effect, with higher values associated with increased vulnerability. The proportion of rental units has a mixed effect and can either increase or decrease the indicator, depending on the tract.

3.5. Assessment of the effects of social vulnerability indicators on exposure using the GWR model

To assess the impact of social vulnerability indicators on exposure in Masjed Soleyman, the geographically weighted regression (GWR) model was employed. Table 7 presents the model's

statistical indicators, while Table 8 shows the local coefficients of the explanatory variables, indicating the direction and magnitude of each variable's effect.

Table 7. Statistical Indicators of the GWR Model

Model Indicator	Value
Bandwidth	4957.22
Residual Sum of Squares (RSS)	0.0662
Effective Number of Parameters	11.58
Residual Standard Deviation (Sigma)	0.0339
Corrected Akaike Information Criterion (AICc)	-258.88
Coefficient of Determination (R^2)	0.536
Adjusted R^2	0.450

Table 8. Local Coefficients of the GWR Model Examining the Effects of Social Vulnerability Indicators on Exposure

Variable	Coefficient Direction	Coefficient Range	Notes
Household Density	Positive / Negative	-0.0072 – 0.4156	The effect of household density varies across census tracts; in some areas, higher density increases the indicator, while in others it decreases it.
Illiteracy Rate	Negative	-0.0055 – -0.0018	Higher illiteracy generally decreases the exposure indicator across most tracts.
Unemployment Rate	Positive	0.00003 – 0.482	Higher unemployment increases the exposure indicator.
Proportion of Rental Units	Positive / Negative	-0.342 – 0.298	Mixed effect; in some tracts, an increase in rental units decreases the indicator, while in others it increases it.

The GWR results indicate that areas with higher social vulnerability show notable variation in the exposure indicator, suggesting a significant spatial relationship between social conditions and exposure levels. In this model, the dependent variable is the exposure indicator at the census tract level. In contrast, the independent variables include household density, illiteracy rate, unemployment rate, and the proportion of rental housing units.

The model explained about 53% of the spatial variation in the exposure indicator ($R^2 = 0.536$), and the adjusted R^2 (0.450) indicates a good fit after accounting for the number of variables.

The indicator coefficients reflect the varying effects of social variables. Household density shows both positive and negative effects across census tracts, indicating local variation in its impact on the exposure indicator. Illiteracy generally has a negative effect in most tracts, with higher illiteracy decreasing the exposure indicator. Unemployment shows a positive effect, with higher unemployment associated with increased exposure. The proportion of rental units has a mixed effect and can either decrease or increase the indicator, depending on the tract.

Areas with higher social challenges—such as high household density, unemployment, illiteracy, and a high proportion of rental units—simultaneously exhibit higher exposure or physical vulnerability indicators. This suggests that social weaknesses contribute to increased urban vulnerability or exposure.

4. Discussion

This study examined social vulnerability and the exposure indicator of Masjed Soleyman, a multi-hazard city, using multi-criteria decision-making (MCDM) techniques and geographically weighted regression. The study analyzed four hazards—floods, earthquakes, landslides, and human-induced

hazards (oil pollution)—along with four physical indicators and nine social vulnerability indicators to provide a comprehensive multi-hazard assessment.

The results indicated that the central and southern parts of the city have the highest hazard exposure, with the exposure indicator peaking in these areas. At the same time, the northern and northwestern regions show the lowest exposure levels. The assessment of physical vulnerability revealed that areas with higher physical vulnerability are scattered across the city without a clear concentration. In contrast, social vulnerability is primarily concentrated in the central and northern parts of the city.

Geographically weighted regression (GWR) analysis revealed that social indicators, including household density, illiteracy rate, unemployment rate, and the proportion of rental units, significantly affect both the exposure and physical vulnerability indicators. Areas with poorer social conditions are simultaneously more physically vulnerable and more exposed to hazards. This spatial and social correlation pattern is clearly observable across different parts of the city.

The results of the composite risk indicator also showed that the central neighborhoods exhibit the highest combined risk, whereas the northwestern and eastern neighborhoods display the lowest risk levels. These findings emphasize that reducing urban vulnerability and improving risk management in Masjed Soleyman require simultaneous attention to social weaknesses, focusing on enhancing social conditions, education, employment, household structure, and housing ownership.

The multi-hazard nature of Masjed Soleyman has been confirmed in previous studies(Arvin et al., 2023; Hejazi et al., 2022). In line with other studies (e.g., Alikaei et al., 2023), the intensity of single and multiple hazards was examined in the present research.

The findings from the geographically weighted regression model indicate a significant spatial relationship between social indicators and urban exposure in Masjed Soleyman. Overall, areas with poorer social conditions are more exposed to urban hazards. This result suggests that social inequalities not only affect quality of life but also influence spatial resilience and the physical safety of neighborhoods.

The predominantly positive coefficients of indicators such as unemployment rate, illiteracy, household density, and the high proportion of rental units indicate that social vulnerability and physical exposure operate in a concurrent and reinforcing spatial pattern. This is particularly evident in neighborhoods with high population density and a greater prevalence of rental housing, where weaknesses in social and economic capital have led to reduced adaptive capacity and increased susceptibility to hazards.

The relationship between social vulnerability and both exposure and physical vulnerability can be interpreted as a risk reproduction cycle. Social weaknesses such as unemployment and illiteracy reduce households' capacity to improve their living environment, gradually creating a more physically vulnerable urban structure. Conversely, residing in high-risk areas further exacerbates poverty and social inequality, thereby perpetuating this cycle.

The model results indicate that the effects of social and economic indicators vary across census tracts, with their magnitude differing between areas. This spatial heterogeneity highlights the importance of place-based policymaking, suggesting that risk reduction programs should be tailored to the social, economic, and structural conditions of each tract.

Following the multi-hazard (aggregate, cascading, and compound) classification, the multi-hazard assessment performed in this research was placed under the aggregate category(Drakes & Tate, 2022a). This approach describes the cumulative effects of multiple independent events. Hazards such as landslides and oil pollution occur in Masjed Soleyman without any connection with each other. Social vulnerability assessment in this category also takes into consideration the existing conditions of the city residents. Previous studies have not conducted social and Physical vulnerability assessments as a multi-hazard analysis at the urban scale, and few studies have combined these two measures. This gap may indicate the need for more research and a more integrated perspective to better understand the mixed effects of social and Physical vulnerability in exposure to hazards. Thus, the present research has sought to fill this gap, and the findings revealed the degree of exposure in different parts of the

city, along with the degree of impact and sensitivity of the population and exposed Physical fabric. (Drakes & Tate, 2022a) considered social vulnerability to be the different conditions of the community that are at risk to a similar extent. However, the data in this research indicated that the populations with different socio-economic conditions living in different census tracts in the city are not similarly exposed to hazards, and they are not threatened by several hazards at the same time.

Masjed Soleyman, as the first oil extraction city in Iran, attracted people from nearby villages and towns, and this trend continues. Residents of nearby villages have migrated to Masjed Soleyman due to the inaccessibility of farming lands and poor economic conditions. These poor migrants have settled in census tracts with steep slopes, slopes with landslides, census tracts with oil and gas contamination, and around oil wells. Their settlement in the elevated census tracts of the city does not comply with geomorphological and risk management criteria. Thus, the people affected by hazards have occupied a large area of the city due to inefficient urban planning(Waly et al., 2021). One of the most important reasons for people living in hazardous areas is the lack of land (Alikaei et al., 2023). In Masjed Soleyman, due to the restrictions and lack of land, people have settled in areas with high slopes and in regions in the vicinity of industries and oil wells.

One of the important issues that has received little attention in previous studies is measuring vulnerability to human hazards. Human hazards such as pollution, fires, and wars cause displacement and many human and financial losses. Oil pollution was addressed as a human hazard in the present. A large number of people live in hazardous areas in Masjed Soleyman for two reasons. Immigrants cannot live in areas with better conditions and far from hazards. Given the geographical conditions of the city, the lowlands and less steep lands are very limited for living, so people are forced to live in hazardous areas. Pollution from oil wells and gas emissions has caused an increase in diseases and casualties. However, these people are not able to move from polluted areas due to unfavorable economic conditions and the government's failure to provide suitable land. Consequently, the higher the rate of social vulnerability in these areas, the more difficult it is to move residents and settle in areas far from hazards and pollution. The government should pay special attention to increasing the number of desirable and safe housing units in areas away from hazards, as well as providing facilities. These measures can increase the ability of residents to move to safer places.

Due to the simultaneous occurrence and sensitivity to four important hazards, i.e., earthquakes, landslides, floods, and oil pollution, Masjed Soleyman faces serious challenges in risk management and sustainable development. These hazards simultaneously affect the city and its residents. Furthermore, the city has a worn-out fabric and marginal areas, which require special attention due to the poverty of the residents and poor living conditions. In addition, buildings in these areas need to be repaired and retrofitted to protect residents from possible risks in the face of natural hazards such as earthquakes and floods. Hence, for the optimal management of hazards and preparation to face these challenges, Masjed Soleyman needs detailed planning, the development of infrastructure resistant to earthquakes and oil pollution, the creation of an effective warning system in the face of floods and landslides, as well as the improvement of living and economic conditions in marginal areas.

A comparison of exposure, Physical vulnerability, and social vulnerability ranks can reveal which areas or communities are exposed to more hazards and thus require emergency preparedness planning and immediate actions. This comparison can help city managers to optimally allocate limited resources. They can also adopt the best strategies for risk management and emergency measures. For example, areas with high exposure and Physical vulnerability may need to strengthen infrastructure and building frames, while communities with high social vulnerability may need social preparedness programs and social actions.

5. Conclusions

This study presented an integrated assessment of social and physical vulnerability in the multi-hazard context of Masjed Soleyman using a three-stage framework that combined GIS, multi-criteria decision-making (MCDM), and geographically weighted regression (GWR). The results showed that

the central and southern parts of the city have the highest concentration of hazards, mainly because of urban decay, population density, and unfavorable geographic conditions.

Using the Best–Worst Method (BWM) and the COCOSO model, we weighted and ranked both social and physical vulnerability indicators. Tracts with higher unemployment, illiteracy, household density, and rental housing rates demonstrated the highest vulnerability. The GWR analysis confirmed that these social weaknesses spatially coincide with areas of high exposure, indicating that social inequalities directly reinforce physical fragility. In other words, disadvantaged neighborhoods are simultaneously more exposed and more vulnerable.

The study's main limitation was the lack of detailed data on factors such as income, insurance, emergency services, and historical hazard records. Future research should integrate these elements, along with dynamic variables like climate change and population mobility, for more comprehensive analyses.

Methodologically, integrating GIS, MCDM, and GWR proved a flexible and cost-effective approach to evaluating urban vulnerability. The findings can support spatial prioritization, disaster risk reduction, and evidence-based planning in developing cities. Ultimately, this study emphasizes that mitigating physical vulnerability requires addressing its social dimensions, aligning with Sustainable Development Goals 11 and 13 toward building safer, more resilient urban environments.

References

Ahmadi, F., Nazeri Tahroudi, M., Mirabbasi, R., & Kumar, R. (2022). Spatiotemporal analysis of precipitation and temperature concentration using PCI and TCI: a case study of Khuzestan Province, Iran. *Theoretical and Applied Climatology*, *149*(1–2), 743–760. https://doi.org/10.1007/s00704-022-04077-6

Aksha, S. K., Resler, L. M., Juran, L., & Carstensen, L. W. (2020a). A geospatial analysis of multi-hazard risk in Dharan, Nepal. *Geomatics, Natural Hazards and Risk*, *11*(1), 88–111. https://doi.org/10.1080/19475705.2019.1710580

Aksha, S. K., Resler, L. M., Juran, L., & Carstensen, L. W. (2020b). A geospatial analysis of multi-hazard risk in Dharan, Nepal. *Geomatics, Natural Hazards and Risk*, *11*(1), 88–111. https://doi.org/10.1080/19475705.2019.1710580

Alam, M. S., Haque, S. M., Alam, M. S., & Haque, S. M. (2018). Assessment of Urban Physical Seismic Vulnerability Using the Combination of AHP and TOPSIS Models: A Case Study of Residential Neighborhoods of Mymensingh City, Bangladesh. *Journal of Geoscience and Environment Protection*, *6*(2), 165–183. https://doi.org/10.4236/GEP.2018.62011

Alikaei, S., Rahmani, M., Jamalabadi, F., Akdogan, M. E., & Khoshnevis, S. (2023). Multi-hazard-based land use planning in isolated area: learning from the experience of Pul-e-Khumri City, Afghanistan. *Sustainable Cities and Society*, *99*, 104873. https://doi.org/10.1016/J.SCS.2023.104873

Alizadeh, M., Alizadeh, E., Kotenaee, S. A., & Shahabi, H. (2018). Social Vulnerability Assessment Using Artificial Neural Network (ANN) Model for Earthquake Hazard in Tabriz City, Iran. *Sustainability*. https://doi.org/10.3390/su10103376

Alizadeh, M., Alizadeh, E., Kotenaee, S. A., Shahabi, H., Pour, A. B., Panahi, M., Bin Ahmad, B., & Saro, L. (2018). Social vulnerability assessment using artificial neural network (ANN) model for earthquake hazard in Tabriz city, Iran. *Sustainability (Switzerland)*, *10*(10), 3376. https://doi.org/10.3390/su10103376

Amini, M., Sanderson, D. R., Cox, D. T., Barbosa, A. R., & Rosenheim, N. (2023). Methodology to incorporate seismic damage and debris to evaluate strategies to reduce life safety risk for multi-hazard earthquake and tsunami. *Natural Hazards*, 1–36. https://doi.org/10.1007/S11069-023-05937-8/METRICS

Araya-Muñoz, D., Metzger, M. J., Stuart, N., Wilson, A. M. W., & Carvajal, D. (2017). A spatial fuzzy logic approach to urban multi-hazard impact assessment in Concepción, Chile. *Science of The Total Environment*, *576*, 508–519. https://doi.org/10.1016/J.SCITOTENV.2016.10.077

Arvin, M., Beiki, P., Hejazi, S. J., Sharifi, A., & Atashafrooz, N. (2023). Assessment of infrastructure resilience in multi-hazard regions: A case study of Khuzestan Province. *International Journal of Disaster Risk Reduction*, *88*, 103601. https://doi.org/10.1016/J.IJDRR.2023.103601

Ba, R., Deng, Q., Liu, Y., Yang, R., & Zhang, H. (2021). Multi-hazard disaster scenario method and emergency management for urban resilience by integrating experiment–simulation–field data. *Journal of Safety Science and Resilience*, *2*(2), 77–89. https://doi.org/10.1016/J.JNLSSR.2021.05.002

Bai, X., Song, K., Liu, J., Mohamed, A. K., Mou, C., & Liu, D. (2019). Health Risk Assessment of Groundwater Contaminated by Oil Pollutants Based on Numerical Modeling. *International Journal of Environmental Research and Public Health, 2019, Vol. 16, Page 3245*, *16*(18), 3245. https://doi.org/10.3390/IJERPH16183245

Banihashemi, A., Khalilzadeh, M., Zavadskas, E. K., Antucheviciene, J., Banihashemi, C. , Khalilzadeh, S. A. , & Zavadskas, M. (2021). Investigating the Environmental Impacts of Construction Projects in Time-Cost Trade-Off Project Scheduling Problems with CoCoSo Multi-Criteria Decision-Making Method. *Sustainability 2021, Vol. 13, Page 10922*, *13*(19), 10922. https://doi.org/10.3390/SU131910922

Bixler, R. P., Yang, E., Richter, S. M., & Coudert, M. (2021). Boundary crossing for urban community resilience: A social vulnerability and multi-hazard approach in Austin, Texas, USA. *International Journal of Disaster Risk Reduction*, *66*, 102613. https://doi.org/10.1016/J.IJDRR.2021.102613

Chakraborty, L., Rus, H., Henstra, D., Thistlethwaite, J., & Scott, D. (2020). A place-based socioeconomic status index: Measuring social vulnerability to flood hazards in the context of environmental justice. *International Journal of Disaster Risk Reduction*, *43*, 101394. https://doi.org/10.1016/J.IJDRR.2019.101394

Chen, C., Zhao, D., He, F., & Sun, F. (2023). A comprehensive multi-hazard risk assessment model for an urban agglomeration with multiple factors. *Journal of Safety Science and Resilience*, *4*(1), 43–51. https://doi.org/10.1016/J.JNLSSR.2022.09.008

De Brito, M. M., Evers, M., & Delos Santos Almoradie, A. (2018). Participatory flood vulnerability assessment: A multi-criteria approach. *Hydrology and Earth System Sciences*, *22*(1), 373–390. https://doi.org/10.5194/hess-22-373-2018

de Loyola Hummell, B. M., Cutter, S. L., & Emrich, C. T. (2016). Social Vulnerability to Natural Hazards in Brazil. *International Journal of Disaster Risk Science*, *7*(2), 111–122. https://doi.org/10.1007/s13753-016-0090-9

Depietri, Y., Dahal, K., & McPhearson, T. (2018). Multi-hazard risks in New York City. *Natural Hazards and Earth System Sciences*, *18*(12), 3363–3381. https://doi.org/10.5194/NHESS-18-3363-2018

Dintwa, K. F., Letamo, G., & Navaneetham, K. (2019). Measuring social vulnerability to natural hazards at the district level in Botswana. *Jamba: Journal of Disaster Risk Studies*, *11*(1). https://doi.org/10.4102/JAMBA.V11I1.447

Drakes, O., & Tate, E. (2022a). Social vulnerability in a multi-hazard context: a systematic review. *Environmental Research Letters*, *17*(3), 033001. https://doi.org/10.1088/1748-9326/AC5140

Drakes, O., & Tate, E. (2022b). Social vulnerability in a multi-hazard context: a systematic review. *Environmental Research Letters*, *17*(3), 033001. https://doi.org/10.1088/1748-9326/AC5140

Ebert, A., Kerle, N., & Stein, A. (2009). Urban social vulnerability assessment with physical proxies and spatial metrics derived from air- and spaceborne imagery and GIS data. *Natural Hazards*, *48*(2), 275–294. https://doi.org/10.1007/S11069-008-9264-0/METRICS

Fang, Z., Liu, Z., Zhao, S., Ma, Y., Li, X., & Gao, H. (2022). Assessment of Groundwater Contamination Risk in Oilfield Drilling Sites Based on Groundwater Vulnerability, Pollution Source Hazard, and Groundwater Value Function in Yitong County. *Water 2022, Vol. 14, Page 628*, *14*(4), 628. https://doi.org/10.3390/W14040628

Fatemi, F., Ardalan, A., Aguirre, B., Mansouri, N., & Mohammadfam, I. (2017). Social vulnerability indicators in disasters: Findings from a systematic review. *International Journal of Disaster Risk Reduction*, *22*, 219–227. https://doi.org/10.1016/J.IJDRR.2016.09.006

Ferreira, T. M., & Santos, P. P. (2023). *An Introduction to Multi-hazard Risk Interactions Towards Resilient and Sustainable Cities*. 1–14. https://doi.org/10.1007/978-981-99-0745-8_1

Gentile, R., Cremen, G., Galasso, C., Jenkins, L. T., Manandhar, V., Menteşe, E. Y., Guragain, R., & McCloskey, J. (2022). Scoring, selecting, and developing physical impact models for multi-hazard risk assessment. *International Journal of Disaster Risk Reduction*, *82*, 103365. https://doi.org/10.1016/J.IJDRR.2022.103365

Ghajari, Y. E., Alesheikh, A. A., Modiri, M., Hosnavi, R., & Abbasi, M. (2017). Spatial Modeling of Urban Physical Vulnerability to Explosion Hazards Using GIS and Fuzzy MCDA. *Sustainability, 2017, Vol. 9, Page 1274*, *9*(7), 1274. https://doi.org/10.3390/SU9071274

Guo, S., Zhang, W., & Gao, X. (2020). Business Risk Evaluation of Electricity Retail Company in China Using a Hybrid MCDM Method. *Sustainability 2020, Vol. 12, Page 2040*, *12*(5), 2040. https://doi.org/10.3390/SU12052040

Hadipour, V., Vafaie, F., & Kerle, N. (2020). An indicator-based approach to assess social vulnerability of coastal areas to sea-level rise and flooding: A case study of Bandar Abbas city, Iran. *Ocean & Coastal Management*, *188*, 105077. https://doi.org/10.1016/J.OCECOAMAN.2019.105077

Hejazi, S. J., Sharifi, A., & Arvin, M. (2022). Assessment of social vulnerability in areas exposed to multiple hazards: A case study of the Khuzestan Province, Iran. *International Journal of Disaster Risk Reduction*, *78*, 103127. https://doi.org/10.1016/J.IJDRR.2022.103127

Highfield, W. E., Peacock, W. G., & Van Zandt, S. (2014). Mitigation Planning. *Http://Dx.Doi.Org/10.1177/0739456X14531828*, *34*(3), 287–300. https://doi.org/10.1177/0739456X14531828

Ikram, Q. D., Jamalzi, A. R., Hamidi, A. R., Ullah, I., & Shahab, M. (2023). Flood risk assessment of the population in Afghanistan: A spatial analysis of hazard, exposure, and vulnerability. *Natural Hazards Research*. https://doi.org/10.1016/J.NHRES.2023.09.006

Jena, R., Pradhan, B., & Beydoun, G. (2020). Earthquake vulnerability assessment in Northern Sumatra province by using a multi-criteria decision-making model. *International Journal of Disaster Risk Reduction*, *46*, 101518. https://doi.org/10.1016/J.IJDRR.2020.101518

Kalaycıoğlu, M., Kalaycıoğlu, S., Çelik, K., Christie, R., & Filippi, M. E. (2023). An analysis of social vulnerability in a multi-hazard urban context for improving disaster risk reduction policies: The case of Sancaktepe, İstanbul. *International Journal of Disaster Risk Reduction*, *91*, 103679. https://doi.org/10.1016/J.IJDRR.2023.103679

Kappes, M. S., Papathoma-Köhle, M., & Keiler, M. (2012). Assessing physical vulnerability for multi-hazards using an indicator-based methodology. *Applied Geography*, *32*(2), 577–590. https://doi.org/10.1016/J.APGEOG.2011.07.002

Karami, S., Mousavi, S. M., & Antucheviciene, J. (2023). Enhancing Contractor Selection Process by a New Interval-Valued Fuzzy Decision-Making Model Based on SWARA and CoCoSo Methods. *Axioms 2023, Vol. 12, Page 729*, *12*(8), 729. https://doi.org/10.3390/AXIOMS12080729

Kassiri, H., Kasiri, A., & Fardin-Mohammadjani, M. (2014). A cross-sectional study on scorpionism in Masjed Soleyman County, Southwestern Iran. *Journal of Entomology*, *11*(4), 238–247. https://doi.org/10.3923/JE.2014.238.247

Khan, S. U., Qureshi, M. I., Rana, I. A., & Maqsoom, A. (2019). An empirical relationship between seismic risk perception and physical vulnerability: A case study of Malakand, Pakistan. *International Journal of Disaster Risk Reduction*, *41*, 101317. https://doi.org/10.1016/J.IJDRR.2019.101317

Khavarian-Garmsir, A. R., Pourahmad, A., Hataminejad, H., & Farhoodi, R. (2019). Climate change and environmental degradation and the drivers of migration in the context of shrinking cities: A case study of Khuzestan province, Iran. *Sustainable Cities and Society*, *47*. https://doi.org/10.1016/j.scs.2019.101480

Lee, Y. J. (2014). Social vulnerability indicators as a sustainable planning tool. *Environmental Impact Assessment Review*, *44*, 31–42. https://doi.org/10.1016/J.EIAR.2013.08.002

Malakar, S., & Rai, A. K. (2023). Estimating seismic vulnerability in West Bengal by AHP-WSM and AHP-VIKOR. *Natural Hazards Research*. https://doi.org/10.1016/J.NHRES.2023.06.001

Malekian, A., & Azarnivand, A. (2016). Application of Integrated Shannon's Entropy and VIKOR Techniques in Prioritization of Flood Risk in the Shemshak Watershed, Iran. *Water Resources Management*, *30*(1), 409–425. https://doi.org/10.1007/S11269-015-1169-6/METRICS

Mengal, A., Goda, K., Ashraf, M., & Murtaza, G. (2021). Social vulnerability to seismic-tsunami hazards in district Gwadar, Balochistan, Pakistan. *Natural Hazards*, *108*(1), 1159–1181. https://doi.org/10.1007/S11069-021-04724-7/METRICS

Mitra, R., & Das, J. (2022). A comparative assessment of flood susceptibility modelling of GIS-based TOPSIS, VIKOR, and EDAS techniques in the Sub-Himalayan foothills region of Eastern India. *Environmental Science and Pollution Research 2022 30:6*, *30*(6), 16036–16067. https://doi.org/10.1007/S11356-022-23168-5

Mladineo, N., Mladineo, M., Benvenuti, E., Kekez, T., & Nikolić, Ž. (2022). Methodology for the Assessment of Multi-Hazard Risk in Urban Homogenous Zones. *Applied Sciences 2022, Vol. 12, Page 12843*, *12*(24), 12843. https://doi.org/10.3390/APP122412843

Morales, F., & Vries, W. T. de. (2021). Establishment of Land Use Suitability Mapping Criteria Using Analytic Hierarchy Process (AHP) with Practitioners and Beneficiaries. *Land 2021, Vol. 10, Page 235*, *10*(3), 235. https://doi.org/10.3390/LAND10030235

Mousavi, S., Geology, M. R.-A. A., & 2020, undefined. (n.d.). The zonation and assessment of slope instability hazard in Masjed Soleyman city using analytical hierarchy process and frequency ratio methods. *Aag.Scu.Ac.IrSS Mousavi, M RahimiAdvanced Applied Geology, 2020•aag.Scu.Ac.Ir*. Retrieved October 18, 2023, from https://aag.scu.ac.ir/article_15867.html?lang=en

Pourghasemi, H. R., Gayen, A., Edalat, M., Zarafshar, M., & Tiefenbacher, J. P. (2020). Is multi-hazard mapping effective in assessing natural hazards and integrated watershed management? *Geoscience Frontiers*, *11*(4), 1203–1217. https://doi.org/10.1016/J.GSF.2019.10.008

Rusk, J., Maharjan, A., Tiwari, P., Chen, T. H. K., Shneiderman, S., Turin, M., & Seto, K. C. (2022). Multi-hazard susceptibility and exposure assessment of the Hindu Kush Himalaya. *Science of The Total Environment*, *804*, 150039. https://doi.org/10.1016/J.SCITOTENV.2021.150039

Saadat, M., Bahaoddini, A., Mohabatkar, H., & Noemani, K. (2004). High incidence of suicide by burning in Masjid-i-Sulaiman (southwest of Iran), a polluted area with natural sour gas leakage. *Burns*, *30*(8), 829–832. https://doi.org/10.1016/j.burns.2004.06.003

Saadat, M., Zendeh-Boodi, Z., & Ali Goodarzi, M. (2006). Environmental exposure to natural sour gas containing sulfur compounds results in elevated depression and hopelessness scores. *Ecotoxicology and Environmental Safety*, *65*(2), 288–291. https://doi.org/10.1016/j.ecoenv.2005.07.024

Safari, H. O., Pirasteh, S., Pradhan, B., & Gharibvand, L. K. (2010). Use of remote sensing data and GIS tools for seismic hazard assessment for shallow oilfields and its impact on the settlements at Masjed-i-Soleiman area, Zagros Mountains, Iran. *Remote Sensing*, *2*(5), 1364–1377. https://doi.org/10.3390/rs2051364

Sani, R. M., Shotorbani, P. M., & Doratli, N. (2015). Exploring the semiotic meaning of the first oil city in the Middle East: Masjed Soleyman. *Social Semiotics*, *25*(3), 342–363. https://doi.org/10.1080/10350330.2015.1021552

Santos-Reyes, J. (2020). Multi-hazard Awareness, Risk Perception and Fear to Earthquakes: The Case of High-school Students in Mexico City. *Journal of Risk Analysis and Crisis Response*, *10*(3). https://doi.org/10.2991/jracr.k.200923.001

Sevieri, G., Galasso, C., D'Ayala, D., De Jesus, R., Oreta, A., Grio, M. E. D. A., & Ibabao, R. (2020). A multi-hazard risk prioritisation framework for cultural heritage assets. *Natural Hazards and Earth System Sciences*, *20*(5), 1391–1414. https://doi.org/10.5194/NHESS-20-1391-2020

Shadmaan, M. S., & Popy, S. (2023). An assessment of earthquake vulnerability by multi-criteria decision-making method. *Geohazard Mechanics*, *1*(1), 94–102. https://doi.org/10.1016/j.ghm.2022.11.002

Soldati, A., Chiozzi, A., Nikolić, Ž., Vaccaro, C., & Benvenuti, E. (2022). A PROMETHEE Multiple-Criteria Approach to Combined Seismic and Flood Risk Assessment at the Regional Scale. *Applied Sciences 2022, Vol. 12, Page 1527*, *12*(3), 1527. https://doi.org/10.3390/APP12031527

Tasnuva, A., Hossain, M. R., Salam, R., Islam, A. R. M. T., Patwary, M. M., & Ibrahim, S. M. (2021). Employing social vulnerability index to assess household social vulnerability of natural hazards: an evidence from southwest coastal Bangladesh. *Environment, Development and Sustainability*, *23*(7), 10223–10245. https://doi.org/10.1007/S10668-020-01054-9/METRICS

Thakur, D. A., & Mohanty, M. P. (2023). A synergistic approach towards understanding flood risks over coastal multi-hazard environments: Appraisal of bivariate flood risk mapping through flood hazard, and socio-economic-cum-physical vulnerability dimensions. *Science of The Total Environment*, *901*, 166423. https://doi.org/10.1016/J.SCITOTENV.2023.166423

Thakur, P. K., Maiti, S., Kingma, N. C., Hari Prasad, V., Aggarwal, S. P., & Bhardwaj, A. (2012). Estimation of structural vulnerability for flooding using geospatial tools in the rural area of Orissa, India. *Natural Hazards*, *61*(2), 501–520. https://doi.org/10.1007/s11069-011-9932-3

Waly, N. M., Ayad, H. M., & Saadallah, D. M. (2021). Assessment of spatiotemporal patterns of social vulnerability: A tool to resilient urban development Alexandria, Egypt. *Ain Shams Engineering Journal*, *12*(1), 1059–1072. https://doi.org/10.1016/J.ASEJ.2020.07.025

Xofi, M., Domingues, J. C., Santos, P. P., Pereira, S., Oliveira, S. C., Reis, E., Zêzere, J. L., Garcia, R. A. C., Lourenço, P. B., & Ferreira, T. M. (2022). Exposure and physical vulnerability indicators to assess seismic risk in urban areas: a step towards a multi-hazard risk analysis. *Geomatics, Natural Hazards and Risk*, *13*(1), 1154–1177. https://doi.org/10.1080/19475705.2022.2068457

Yariyan, P., Karami, M. R., & Ali Abbaspour, R. (2019). EXPLOITATION OF MCDA TO LEARN THE RADIAL BASE NEURAL NETWORK (RBFNN) AIM PHYSICAL AND SOCIAL VULNERABILITY ANALYSIS VERSUS THE EARTHQUAKE (CASE STUDY: SANANDAJ CITY, IRAN). *The International Archives of the Photogrammetry, Remote Sensing and Spatial Information Sciences*, *XLII-4-W18*(4/W18), 1071–1078. https://doi.org/10.5194/ISPRS-ARCHIVES-XLII-4-W18-1071-2019

Zhang, T., Wang, D., & Lu, Y. (2023). Machine learning-enabled regional multi-hazards risk assessment considering social vulnerability. *Scientific Reports 2023 13:1*, *13*(1), 1–14. https://doi.org/10.1038/s41598-023-40159-9

Zou, Q., Cui, P., Zhang, Z., Sijimons, K., Titti, G., Li, S., & Jiang, H. (2022). A novel approach of multi-hazard integrated zonation on the ancient Silk Road. *International Journal of Disaster Risk Reduction*, *82*, 103325. https://doi.org/10.1016/J.IJDRR.2022.103325